

Transfection of mu MDR 1 Inhibits Na⁺-Independent Cl⁻/HCO₃⁻ Exchange in Chinese Hamster Ovary Cells[†]

John Gately Luz,[‡] Li-Yong Wei,[‡] Subham Basu, and Paul D. Roepe*

Program in Molecular Pharmacology & Therapeutics, Memorial Sloan-Kettering Cancer Center, and Graduate School of Medical Sciences, Cornell University, 1275 York Avenue, New York, New York 10021

Received November 29, 1993; Revised Manuscript Received April 11, 1994*

ABSTRACT: We have used single-cell photometry to measure intracellular pH (pH_i) for several MDR cell lines constructed by stably transfecting LR73 chinese hamster ovary fibroblasts with mutant and wild type murine MDR 1 genes. In addition, plasma membrane electrical potential (ΔΨ) has been measured for the same cells by the K⁺/valinomycin null point titration method using the ratiometric styryl probe di-4-ANEPPS. Both the untransfected, parental cell line and a cell line expressing substantial mutant MDR 1 protein (K432R/K1074R) that is unable to confer the MDR phenotype are found to have ΔΨ ≥ -40 (±5) mV and pH_i ≤ 7.16 (±0.03) units. In contrast, MDR cell lines constructed by transfecting wild type mu MDR 1 cDNA are found to exhibit ΔΨ from 15 to 19 mV lower and pH_i from 0.13 to 0.34 units higher. A cell line that overexpresses crippled MDR protein (S941F) that is not resistant to colchicine or doxorubicin, but which is resistant to vinblastine [Gros, P., Dhir, R., Croop, J., & Talbot, F. (1991) *Proc. Natl. Acad. Sci. U.S.A.* 88, 7289-7293], exhibits elevated pH_i and slightly elevated ΔΨ, relative to LR73. Northern and western blot analyses confirm the substantial overexpression of the mu MDR genes and proteins in these lines, as well as the mild overexpression of endogenous hamster p-GP mRNA in some lines. In general agreement with previous studies that examined myeloma cells overexpressing hu MDR 1 protein [Roepe, P. D., Wei, L.-Y., Cruz, J., & Carlson, D. (1993) *Biochemistry* 32, 11042-11056] we find that overexpression of wild type mu MDR 1 protein inhibits Cl⁻- and HCO₃⁻-dependent pH_i homeostasis. Via single-cell photometry studies we now conclude that this is due to inhibition of Na⁺-independent Cl⁻/HCO₃⁻ exchange (strict anion exchange or AE). As concluded previously for other MDR cells, decreased AE activity is not due to decreased expression of the exchanger; in fact, again similar to previous work [Roepe *et al.* (1993) *Biochemistry* 32, 11042-11056], we find *increased* levels of AE mRNA in some MDR cell lines. Models that may explain these data that are also consistent with the known physiology of cells that endogenously express MDR protein are suggested. These data are consistent with a model for MDR protein function wherein overexpression of the protein decreases ΔΨ and/or elevates pH_i via Cl⁻- and HCO₃⁻-dependent mechanisms.

Upon continued selection in one of a variety of chemotherapeutics, some tumor cells will develop multidrug resistance (MDR)¹ which is characterized by a rather broad resistance to, and decreased retention of, chemotherapeutics and other hydrophobic compounds that are usually weakly basic and thus cationic at physiologic pH (Biedler & Rhiem, 1970; Beck, 1987; Gottesman & Pastan, 1988; Endicott & Ling, 1989; Hammond *et al.*, 1989). MDR is often, but not always (Cole *et al.*, 1992), due at least in part to overexpression of the MDR protein, or P-glycoprotein (p-GP). The MDR protein shares considerable homology with other members of

the ABC family of transporters (Ames, 1986; Higgins *et al.*, 1990), which includes the cystic fibrosis transmembrane conductance regulator (CFTR), the multidrug-resistance-related protein [MRP; see Cole *et al.* (1992)], the hly B, mal K, and his P proteins of *Escherichia coli*, the STE 6 pheromone transporter from *Saccharomyces cerevisiae*, and the chloroquine resistance proteins from the malarial parasite *Plasmodium falciparum*.

p-GP is believed by many investigators to contribute to tumor MDR by actively exporting the wide variety of structurally divergent compounds to which MDR cells are resistant (i.e., it is believed to be the first example of a multisubstrate active efflux pump). Since active transporters are in general exquisitely specific with regard to what they transport, a basic conundrum surrounding this model is the lack of substrate specificity. An alternative potential explanation has recently been proposed wherein the documented Cl⁻ translocating ability of the protein (Valverde *et al.*, 1992; Gill *et al.*, 1992; Altenberg *et al.*, 1994) leads to altered plasma membrane electrical potential (ΔΨ) and/or intracellular pH (pH_i). These alterations are envisioned to indirectly promote decreased retention of chemotherapeutics over time by several different mechanisms (Roepe, 1992; Roepe *et al.*, 1993), and they are thus expected to confer broad resistance to a wide variety of hydrophobic, weakly basic/cationic compounds, and/or compounds that bind to intracellular targets in a highly pH dependent manner. These alterations are also expected in some cases to contribute to a variety of other phenomena

[†] This research was supported by grants from the Raymond & Beverly Sackler Foundation, the Society of Sloan-Kettering, and a Cancer Center Support Grant (NCI-P30-CA-08748).

* To whom correspondence should be addressed.

[‡] These two authors contributed equally to this study; thus this sequence is arbitrary.

© Abstract published in *Advance ACS Abstracts*, May 15, 1994.

¹ Abbreviations: MDR, multidrug resistance; p-GP, P-glycoprotein; ΔΨ, plasma membrane electrical potential; pH_i, intracellular pH; Δμ_{H⁺}, plasma membrane electrochemical potential (Δμ_{H⁺} = ΔΨ + ΔpH); AE, anion exchange; SSC, 150 mM sodium chloride/15 mM sodium citrate; PMSF, phenylmethanesulfonyl fluoride; BSA, bovine serum albumin; HEPES, N-(2-hydroxyethyl)piperazine-N'-2-ethanesulfonic acid; BCECF, 2',7'-bis(carboxyethyl)-5(6)-carboxyfluorescein; SNARF, carboxy-semi-naphthorhodafleur-1; di-4-ANEPPS, a (dialkylamino)naphthalene pyridinium styryl dye; SITS, 4-acetamido-4'-isothiocyanatostilbene-2,2'-disulfonic acid; AE, Cl⁻/HCO₃⁻ exchange (anion exchange); Na⁺/AE, Na⁺/Cl⁻/2-HCO₃⁻ cotransport (Na⁺-coupled anion exchange); NHE, Na⁺/H⁺ exchange.

sometimes seen in MDR cells (including altered signal transduction and protein phosphorylation), and they more easily explain the curious resistance MDR cells exhibit to ionophores, which kill cells in a $\Delta\mu_{H^+}$ -dependent manner. Consistent with the altered $\Delta\Psi/pH_i$ hypothesis are many observations of elevated pH_i (Keizer & Joenje, 1989; Boscoboinik *et al.*, 1990; Thiebaut *et al.*, 1990; Roepe, 1992; Wei & Roepe, 1994) as well as lowered pH_i (Altenberg *et al.*, 1993) in MDR cells, and recent quantitative estimates of $\Delta\Psi$ in a series of MDR cells expressing variable MDR protein (Roepe *et al.*, 1993), as well as the well-known importance of Cl^- concentration and Cl^- permeability in maintaining these parameters. Thus, increased plasma membrane Cl^- permeability mediated by MDR protein could lead to decreased $\Delta\Psi$ as is the case with CFTR [see Stutts *et al.* (1993)] and might contribute to altered pH_i by perturbing normal Cl^-/HCO_3^- exchange and/or the character of plasma membrane $\Delta\mu_{H^+}$ (Roepe *et al.*, 1992, 1993).

A third possibility, implied but not proven by the data of Higgins, Sepúlveda, and co-workers (Gill *et al.*, 1992) is that both mechanisms (i.e., active drug transport and altered $pH_i/\Delta\Psi$) contribute to the MDR phenotype. This model rests on the proposal (Gill *et al.*, 1992) that MDR protein functions as both a Cl^- channel and a multisubstrate active drug transporter.

In previous work (Roepe, 1992; Roepe *et al.*, 1993) we studied the relationships between MDR, elevated pH_i , and lowered $\Delta\Psi$ for human MDR myeloma cells created by selection on doxorubicin (Dalton *et al.*, 1989). To test the importance of these trends in the MDR phenotype, we have now analyzed the characteristics of a series of MDR cell lines previously created by transfecting LR73 chinese hamster ovary fibroblasts with either wild type or mutant mu MDR 1 genes under control of the adenoviral promoter/SV40 enhancer (Azzaria *et al.*, 1989; Devault & Gros, 1990; Gros *et al.*, 1991). Our data strengthen the correlations between MDR and decreased $\Delta\Psi$ and elevated pH_i and thus support the "one-two punch" model for MDR protein function (Roepe *et al.*, 1993). They also help to define the molecular-level defects in MDR cells that may lead to elevated pH_i .

MATERIALS AND METHODS

Materials. 2',7'-Bis(carboxyethyl)-5(6)-carboxyfluorescein (BCECF), carboxy-seminaphthorhodafluor-1 (SNARF), nigericin, valinomycin, and the (dialkylamino)naphthalene pyridinium styryl dye di-4-ANEPPS were purchased from Molecular Probes (Eugene, OR) and used without further purification. 4-Acetamido-4'-isothiocyanatostilbene-2,2'-disulfonic acid (SITS) and amiloride were from Sigma. [^{14}C]-Inulin and 3H_2O were from New England Nuclear; the high molecular weight fraction of inulin was purified before use by passage over a Sephadex G-50 column. All other chemicals were reagent grade or better, purchased from commercial sources, and used without further purification.

Tissue Culture. Construction of the cell lines used in this work has been described previously (Azzaria *et al.*, 1989; Devault & Gros, 1990; Gros *et al.*, 1991). In brief, all cell lines were created by simultaneously transfecting two plasmid constructs, one harboring a neomycin resistance gene, and the other the mu MDR 1 gene [mixed at a 1:10 ratio; see Devault and Gros (1990)]. Thus transfectants were initially selected with G418. In some cases (the IF5/9 and 1-1 cell lines), surviving colonies were further selected on vinblastine (25 and 50 ng/mL, respectively), which increases MDR gene expression as evidenced by northern and western blot (see

Results), but which may complicate analysis of the MDR cell's resistance profile by inducing other resistance mechanisms that may or may not be specific to vinblastine. In contrast, the EX4N7 and 88-8 cell lines, harboring WT MDR 1 and K432R/K1074R MDR 1, respectively, were selected on G418 only. In Results, we state that some cells also express increased endogenous hamster p-GP mRNA, which might subtly complicate analysis in some cases. However, in all cases mu MDR mRNA levels were found to be substantially higher than hamster p-GP mRNA levels (see Results).

Cells were grown at 37 °C in a 5% CO_2 atmosphere in DME medium supplemented with 100 units/mL penicillin and 100 μ g/mL streptomycin. EX4N7 and 88-8 were grown in the presence of 500 μ g/mL G418 (Sigma), and IF5/9 and 1-1 were grown in the presence of 25 and 50 ng/mL vinblastine, respectively. For $\Delta\Psi$ measurements (see below), they were harvested by trypsinization, washed, and gently resuspended in fresh media. For northern and western blot analysis the cells were harvested by either trypsinization or scrapping with a sterile rubber policeman.

For single-cell photometry analysis of pH_i , the cells were grown as above on glass coverslips (Corning Glassworks, 18 mm²/0.11 mm thick) that were immobilized in standard tissue culture plates with a dab of autoclaved silicon vacuum grease (Dow-Corning). Cells grown on coverslips were kept in media at 37 °C and 5% CO_2 until immediately before mounting on a perfusion chamber (see below). The perfusion chamber was tooled by the Sloan-Kettering medical physics laboratory after a design kindly provided by Dr. Larry Palmer, Department of Physiology & Biophysics, Cornell Medical College. The chamber provides for unilamellar flow of perfusate over an elliptical surface area of about 3 cm². After mounting, cells were immediately perfused with 37 °C HBSS containing 10 mM glucose that had been previously equilibrated with 5% CO_2 (see single-cell photometry, below).

Drug Resistance. Resistance to chemotherapeutics was assayed by a growth inhibition assay using 96-well plates and crystal violet staining to assess cell density (Prochaska & Santamaria, 1988). Control cell number vs dye absorbance plots verified that staining was a linear function of cell density over the range examined (0.15–1.50 OD). Cells were plated (2×10^4 /well) and allowed to attach overnight. They were then grown at 37 °C and 5% CO_2 on increasing concentrations of drug for 3–4 days, at which point the plates were stained and relative survivability was calculated.

Isolation of mRNA and Northern Blot Analysis. Total cellular RNA was isolated by the method of Chomczynski and Sacchi (1987). Poly (A⁺) RNA was selected by passing total RNA dissolved in 0.5 M NaCl/20 mM Tris/1 mM EDTA/0.1% sarcosyl, pH 7.6, through an oligo(dT)-cellulose column and eluting with 10 mM Tris/1 mM EDTA/0.05% SDS, pH 7.6, as described (Sambrook *et al.*, 1989).

Poly (A⁺) RNA (5 μ g) was denatured with formaldehyde, size-fractionated by 1.2% agarose gel electrophoresis, and subsequently transferred to a nylon membrane filter (Schleicher & Schuell, Keene, NH) by capillary blotting. Membranes were prehybridized in 6 \times SSC/2 \times Denhardt's/0.1% SDS for 4 h at 68 °C and hybridized at the same temperature overnight with labeled probe in 6 \times SSC/0.5% SDS/100 μ g/mL denatured salmon sperm DNA. Probes, isolated from MDR, AE 1, AE 2, β -actin, or rPO cDNAs as described (Roepe *et al.*, 1993), were labeled by the random priming method and purified by passage through a Sephadex G-50 spin column before use. Blots were washed once at room temperature in 2 \times SSC for 20 min, twice at 68 °C in 0.2

\times SSC/0.5% SDS for 30 min, and then two to three times more at 68 °C in 0.1 \times SSC/0.5% SDS for 30 min before imaging radioactivity. Blots probed more than once were stripped by washing at 88 °C in 0.1 \times SSC/0.5% SDS for 3 h. Bands were visualized either by autoradiography (we used Kodak X-OMAT AR film; exposure times varied between 4 and 16 h, see captions) or by imaging β radiation with a betascope 603 blot analyzer (Betagen). For quantitative imaging, bands of interest were first normalized relative to background emission detected by the betascope. To calculate relative levels of AE or MDR mRNA, the signal from a given mRNA preparation was normalized relative to the signals for β -actin and acidic ribosomal phosphoprotein PO (rPO) (see Results). The ratio of β -actin/rPO band intensities was the same for each cell line, in multiple mRNA preparations and multiple northern blots.

Western Blotting. Cells were harvested from a 75-cm² flask after growth at 5% CO_2 to near confluency, washed once in PBS (pH 7.3), snap-frozen with dry ice/ethanol, and stored at -80 °C. Cells were thawed and lysed in 300 μL of cracking buffer (10% glycerol/1% Triton X-100/1 mM PMSF/10 $\mu\text{g}/\text{mL}$ leupeptin/20 mM HEPES). They were then vortexed, incubated at 4 °C for 15 min, and spun in a microcentrifuge (12 000 rpm) at 4 °C for 1 min. The supernatant was removed, and 5 μL was assayed with the Bio-Rad protein assay kit. Total cellular protein, 150 μg , was then resolved by Na-DodSO₄/polyacrylamide gel electrophoresis. Protein was blotted to nitrocellulose (Bio-Rad) at 40-mA constant current overnight at room temperature. Blots were blocked with 5% BSA in TNT buffer (10 mM Tris/0.9% NaCl/0.2% Triton X-100, pH 7.4) for 2 h with shaking at room temperature and then incubated with 20 μL of the monoclonal antibody C219 (0.1 mg/mL) in 10 mL of TNT buffer containing 5% BSA for an additional 2 h at room temperature. After washing three times in TNT buffer, the blot was incubated with 10 μL of horseradish peroxidase labeled anti-mouse IgG (0.1 mg/mL) in 10 mL of TNT for 1 h. After washing, bound antibody was detected by the enhanced chemiluminescence (ECL) method (Amersham) and autoradiography.

Fluorescence Spectroscopy. Fluorescence spectra were obtained with a Photon Technologies Inc. (P.T.I., New Brunswick, NJ) fluorometer interfaced to an AST Research personal computer. Sample cuvettes were jacketed within an aluminum holder, and temperature was controlled by a circulating water bath. Cell suspensions were rapidly mixed with a magnetic stirrer situated beneath the cuvette. Excitation/emission wavelengths and the other parameters of various experiments may be found in the individual figure captions.

Single-Cell Photometry and Measurement of pH_i . We have constructed a single-cell photometry apparatus by interfacing a Nikon diaphot epifluorescence microscope and associated optics to a Photon Technologies Inc. alphascan fluorometer. Excitation was with a xenon lamp directed to a fiber optic cable (P.T.I.) connected to the rear port of the microscope. Excitation was modulated via computer control of the fluorometer's excitation monochromator.

In general, a 0.5-nm slit directed broad band excitation to the fiber optic and hence a 510-nm dichroic mirror positioned beneath the microscope stage that reflected excitation light (≤ 510 -nm wavelength) up through a 40 \times objective (Nikon) and to the cells but passed cell fluorescence longer than 510 nm toward two photon multiplier tubes (PMT) connected in T-format to the side port of the microscope. A 530-nm filter was placed beneath the dichroic, and a second dichroic mirror positioned 45° relative to the plane of each of the two PMT

chambers could be used to detect two emission wavelengths, if desired. Signals from the PMTs were transferred to an AST computer and analyzed with P.T.I. software. ASCII output files were in some cases further analyzed with Sigmaplot software on a Macintosh IICx computer.

Cells were grown on sterile glass coverslips as described above and used >1.5 but <4 days after plating: before confluency but after several cell divisions. Coverslips were incubated with 5 μM acetomethoxy BCECF (BCECF-AM) for 30 min before mounting on the microscope stage, and they were then continuously perfused at a constant rate (approximately 6 mL/min) with buffer equilibrated to 37 °C. Uniform BCECF staining was verified visually and by monitoring the intensity of 490-nm excitation. Buffers harboring HCO_3^- were continuously purged with 5% CO_2 , and a fine jet of 5% CO_2 was directed over the mounted coverslip. Buffer pH was monitored with a microelectrode. Several control experiments verified that leak of the esterified BCECF-AM was miniscule in the time required to make a measurement, and not any different for MDR cells vs their parent. Exposure to excitation light was limited to the time of data collection to limit photobleaching.

To calculate steady-state pH_i , calibration curves were obtained essentially using the K^+ /nigericin titration approach of Thomas and colleagues (1979) as described previously (Roepe 1992; Roepe *et al.*, 1993), but in a "single-cell mode" wherein buffer harboring nigericin was continuously flowed over the cells. 439/490 BCECF excitation ratios (535 emission) were obtained for individual cells perfused with KNH buffer (40 mM KCl/100 mM NaCl/20 mM HEPES/1 μM nigericin) at 37 °C and various pH_o . The ratios from 12 to 20 cells were then averaged and plotted vs known pH_o (equal to pH_i in the presence of the nigericin). The standard curves thus generated for the different cell lines were superimposable (see Results). Multiple 439/490 excitation measurements for cells perfused with physiologic buffers (see Results) in the absence of nigericin were then averaged and pH_i was computed using a quadratic fit to the standard curve (see Results). Standard curves were generated for every coverslip used to make the pH_i measurements under physiologic conditions.

To produce Cl^- -dependent changes in pH_i (" Cl^- substitution" experiments), Cl^- in the perfusate was replaced with equimolar glutamate or gluconate (we did not observe significant differences between experiments performed with the different impermeant anions). After the observed pH_i perturbation began to plateau (within 100–120 s, see Results), normal $[\text{Cl}^-]$ was restored. Perfusate flow was kept constant at 6 mL/min using a peristaltic pump (Pharmacia LKB Model P-1). In some cases, experiments were performed in the absence of HCO_3^- or Na^+ or in the presence of stilbene inhibitors (see appropriate figure captions for additional detail).

Measurement of Electrical Membrane Potential ($\Delta\Psi$). We used the fast response styryl dye di-4-ANEPPS (Montana *et al.*, 1989; Loew *et al.*, 1993) to assess $\Delta\Psi$ due to the fact that it is very well localized to the plasma membrane of the cells used in this study within the time used to make our measurements (P.D.R., unpublished fluorescence microscopy data) and because the measured *ratio* of excitation at 440 and 505 nm when monitoring emission at 610 nm is dependent upon the magnitude of $\Delta\Psi$. Thus, contributions to the measured $\Delta\Psi$ from mitochondria and other organelles as well as variability in the concentration of cell-associated dye are less of a concern, respectively. Since the probe is ratiometric, and since we cannot detect any significant difference in the

Table 1: Steady-State pH_i and Quantitative Estimates of $\Delta\Psi$ for the Series of LR73 Transfectants^a

cell line	pH_i	K^+ /val null point (mM)	$\Delta\Psi$ (mV)	rel drug resistance ^b
LR73	7.16 ± 0.03	28	42	none
88-8	7.12 ± 0.05	31	41	none
EX4N-7	7.29 ± 0.04	62	23	mild MDR
EX4N-7 revertant	7.19 ± 0.04	30	40	none
1-1	7.50 ± 0.06	52	27	very MDR
IF5/9	7.23 ± 0.03	20	52	mild VBL

^a pH_i was determined by single-cell photometry using BCECF (see Materials and Methods) and $\Delta\Psi$ by K^+ /valinomycin null point titration using the styryl dye di-4-ANEPPS (Montana *et al.*, 1989; Roepe *et al.*, 1993). To quantitatively estimate $\Delta\Psi$, K^+ was first estimated (Roepe *et al.*, 1993) by flame-photometry determination of cell-associated K^+ and Coulter sizing/[¹⁴C]inulin partitioning to estimate cell water volume (see Materials and Methods); K^+ was then inserted into the Nernst relation along with null point K^+ (see Figure 4A,B) to estimate $\Delta\Psi$ [see Laris and Hoffman (1986) and Roepe *et al.* (1993)]. It is assumed that K^+ current dominates $\Delta\Psi$ in these cells; this can be qualitatively verified by measuring hyperpolarization and depolarization in the presence of high Na^+ or high K^+ and gramicidin [not shown; see Roepe *et al.* (1993)]. See Figure 4 for representative null point titrations. ^b See Azzaria *et al.* (1989), Devault and Gros (1990), and Gros *et al.* (1991). Cultures of these cell lines used in the present work were analyzed for relative resistance to colchicine, vinblastine, and doxorubicin by growth inhibition (see Materials and Methods); no major differences in resistance pattern were observed, relative to previous work, although fold-resistance to some drugs as calculated by growth inhibition was slightly different relative to fold-resistance calculated by colony formation (Azzaria *et al.*, 1989; Gros *et al.*, 1991).

leak of this dye for MDR vs sensitive cells, any postulated pumping of the dye by p-GP would not, if it even existed, bias the measurements.

$\Delta\Psi$ was calibrated by the null point K^+ /valinomycin titration method of Laris and Hoffman (1986) with HBSS containing 10 mM HEPES, pH 7.30 at 37 °C used as the standard solution and increased $[K^+]_o$ substituting for decreased $[Na^+]_o$. Solutions harboring various $[K^+]_o$ and 0.5 μ M di-4-ANEPPS were rapidly mixed with 5×10^5 cells. Rapid uptake of di-4-ANEPPS into the plasma membrane was monitored (see Results), and after a flat base line was observed valinomycin was added to a final concentration of 10 μ M. The change in the ratio of 440 to 505 nm excitation (610-nm emission) was plotted as a function of external $[K^+]_o$ and the minimum (null point) determined graphically. For each null point titration, three traces were obtained at a given $[K^+]_o$ and then averaged. Five different averaged traces (obtained at five different $[K^+]_o$) were then plotted to determine the null point. Null points obtained from three such plots were then averaged to calculate $\Delta\Psi$ (see Table 1 caption). See Roepe *et al.* (1993) for additional detail.

Measurement of $[K^+]_i$. Cell-associated K^+ was measured by flame photometry as described (Iversen, 1976; Roepe *et al.*, 1993). After determination of intracellular volume (see below), $[K^+]_i$ was calculated.

Measurement of Intracellular Volume (V_i). Total cell volume was calculated after determining the mean particle size of cell suspensions by the single-threshold Coulter method (Kachel, 1990; Roepe *et al.*, 1993). Intracellular water volume was determined by ratioing [¹⁴C]inulin vs ³H₂O dpm as described (Rottenberg, 1979; Roepe *et al.*, 1993).

RESULTS

Single-cell photometry methods have proven invaluable in the analysis of intracellular pH (pH_i) and other phenomena [e.g., Alpern and Chambers (1987) and Weiner and Hamm (1990)]. The method is dependent on the reproducibility of

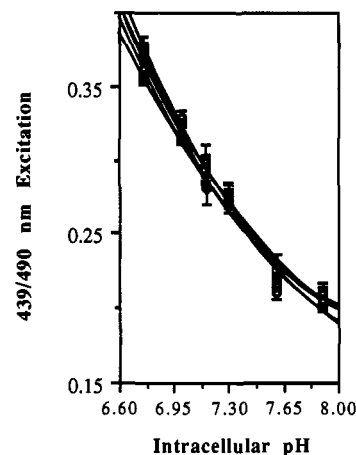


FIGURE 1: BCECF 439/490 nm excitation vs pH_i standard curves for the LR73, 88-8, EX4N7, 1-1, and IF5/9 cell lines used in this work. Each data point represents the average of excitation ratios for 12–20 individual cells from a coverslip that was constantly perfused with KNH buffer at various pH (see Materials and Methods). Each data set was well fitted by a quadratic ($R^2 > 0.95$ in each case). Note that the curves for the different cells have identical slope and are virtually superimposable; thus the pH_i -dependent response of BCECF is identical for each cell line. Thus, any hypothesized interaction of BCECF with the MDR protein (Homolya *et al.*, 1993), if it even exists at all, does not bias our measurements of pH_i for the MDR cells.

the excitation or emission of an ion-responsive probe such as BCECF, which should be rigorously checked in every cell line examined. Thus, in Figure 1 we present BCECF excitation vs pH_i standard curves generated by the K^+ /nigericin method (Thomas *et al.*, 1979), for each of the cell lines used in this work. Note that the curves for the different cell lines have identical slope, and all virtually superimpose, indicating that the pH_i -dependent response of intracellular BCECF is essentially identical for the different cell lines. Since BCECF is a ratiometric probe, these data, along with other experiments (not shown) that show that the rate of esterified BCECF-AM leak from the different cells is indistinguishable ($<1\%$ /min), allow us to conclude that any hypothetical interaction of BCECF with MDR protein, if it occurs at all, does not lead to artifacts that might unduly bias pH_i measurements for the MDR cells. Similar arguments can be used to verify the applicability of the di-4-ANEPPS method for quantitatively estimating $\Delta\Psi$ [see Roepe *et al.* (1993)].

In any case, by analyzing dozens of individual cells by single-cell photometry methods, we find that in the presence of physiologic $[HCO_3^-]$ pH_i is elevated for the EX4N7 and 1-1 cell lines by approximately 0.13 and 0.34 units, respectively, relative to the parental line LR73 (Table 1). Since these lines harbor significant levels of wild type mu MDR 1 protein (Figure 2), these data strengthen the positive relationship between elevated pH_i and increased MDR protein expression noted in previous work (Keizer & Joenje, 1989; Thiebaut *et al.*, 1990; Roepe, 1992). The strongest evidence in favor of the relationship comes from the EX4N7 data, since this cell line was never exposed to chemotherapeutic drugs (see Materials and Methods) and thus additional drug resistance mechanisms that might further perturb pH_i (Roepe *et al.*, 1993) are presumably not induced.

Interestingly, the cell line IF5/9, which expresses a S941F mu MDR 1 mutant (Gros *et al.*, 1991) and which is measurably resistant to vinblastine but not other chemotherapeutics, exhibits a pH_i approximately 0.07 units higher than LR73 (Table 1). Since this measured elevation is close to our limit of detection, care should be used in interpreting

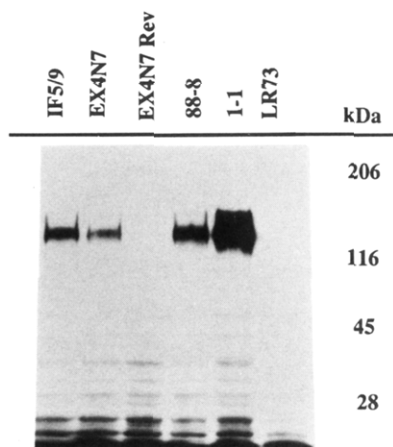


FIGURE 2: Western blot analysis of MDR protein expression for the cell lines used in this work. Each lane harbors 150 μg of total cellular protein (see Materials and Methods), and the monoclonal C219 was used as the primary antibody. The prominent band at about 180 kDa represents mu MDR 1 (note the absence of this band in the LR73 lane). Some cross reactivity of the C219 antibody with low molecular weight proteins is observed when we blot total cellular protein; this background is reduced for some cells when we blot purified membrane protein [see Wei and Roepe (1994)]. Exposure time was approximately 5 min. Northern blot analysis of MDR gene expression in this series reveals substantial overexpression of the mu MDR 1 mRNA (not shown). Other blots using a p-GP 1 specific probe (not shown) indicate that mu MDR 1 mRNA is at least an order of magnitude more prevalent than endogenous p-GP 1 mRNA in the transfectants, and also reveals mild (3–4-fold) overexpression of p-GP 1 for EX4N7 and IF5/9.

its significance. Also, since this cell line was selected on 25 ng/mL vinblastine, it is initially difficult to conclude whether expression of the mutant MDR protein is solely responsible for this mild elevation in pH_i (we note a very mild increase in endogenous hamster p-GP mRNA for IF5/9 by northern blot, data not shown). In any case, in contrast to these data the cell line 88-8, which overexpresses a mu MDR 1 gene harboring two nucleotide binding site K to R mutations (Azzaria *et al.*, 1989; see Figure 2) and which is not resistant to any chemotherapeutics, exhibits a pH_i in the presence of HCO_3^- that is very similar to that of LR73 (Table 1). As a final test, we grew the EX4N7 cell line for 5 months in the constant presence of G418 only, at which point the line reverts and loses all measurable mu MDR protein and mRNA (see Figure 2 and Table 1). The revertant is found to exhibit a pH_i similar to that of LR73 (Table 1).

Previously (Roepe *et al.*, 1993), we also found a strong positive relationship between increased MDR protein expression and decreased plasma membrane electrical potential ($\Delta\Psi$) in a series of MDR myeloma cell lines exhibiting various levels of MDR. As shown in Table 1, those MDR cell lines created by transfection with the wild type mu MDR 1 gene that exhibit elevated pH_i also exhibit decreased $\Delta\Psi$, as measured by K^+ /valinomycin null point titration as described in detail previously (Roepe *et al.*, 1993). See Figure 3 for a comparison of representative null point titrations for the LR73 and EX4N7 cell lines. In contrast, the cell lines 88-8 and IF5/9, which harbor completely or partially crippled MDR proteins, are found to have $\Delta\Psi > -40$ mV (Table 1). Interestingly, the IF5/9 cell line is found to have a slightly higher $\Delta\Psi$ relative to LR73, which might explain why the line is not appreciably resistant to doxorubicin and other chemotherapeutics, even though pH_i is slightly elevated (see Discussion).

We obviously wish to understand how steady-state pH_i is elevated in MDR cells, and whether MDR protein directly plays a role in this phenomenon. In a previous paper (Roepe

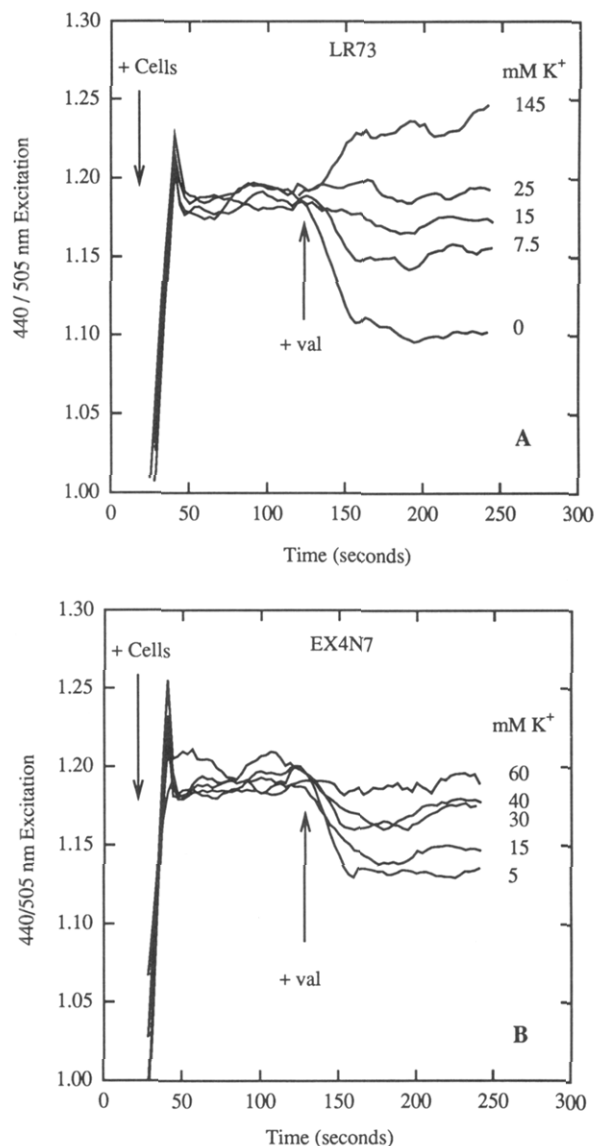


FIGURE 3: Representative K^+ /valinomycin null point titrations for the LR73 (A) and EX4N7 (B) cell lines. Cells (5×10^5) were rapidly mixed with 0.5 μM di-4-ANEPPS in buffer of various $[\text{K}^+]_o$ (first arrow), and valinomycin was added 100 s later to a final concentration of 10 μM (second arrow; see Materials and Methods). Three traces obtained at each $[\text{K}^+]_o$ were averaged, and the result was smoothed with the Savitzky/Golay algorithm (Savitzky & Golay, 1964) using a 15 point buffer. The relative change in 440/505 excitation was determined after fitting the portions of the trace before and after addition of valinomycin to a straight line. After plotting the relative change in 440/505 nm excitation (610-nm emission) vs $[\text{K}^+]_o$, the null point is determined graphically [see Roepe *et al.* (1993)]. The average null point from three such plots is then inserted into the Nernst equation along with estimated $[\text{K}^+]_i$ to determine $\Delta\Psi$ [see also caption to Table 1 and Roepe *et al.* (1993) for additional details]. As noted by Loew and colleagues (Montana *et al.*, 1989; Loew *et al.*, 1993), di-4-ANEPPS excitation ratios are well behaved between 10 and -100 mV. Although the intrinsic difference signal is small, averaging multiple traces provides suitable signal/noise ratios. Since di-4-ANEPPS is a ratiometric probe, a variety of complexities inherent in the use of carbocyanine or oxonol probes are avoided [see Roepe *et al.* (1993)].

et al., 1993) we determined that Cl^- -dependent pH_i homeostasis was perturbed in MDR cells via pH_i recovery experiments using mass populations of MDR myeloma cells. In Figures 4 and 5 we improve upon those data by presenting “ Cl^- -substitution pH_i transients” (see Materials and Methods) recorded using single-cell photometry methods in the absence (Figure 4) or presence (Figure 5) of HCO_3^- .

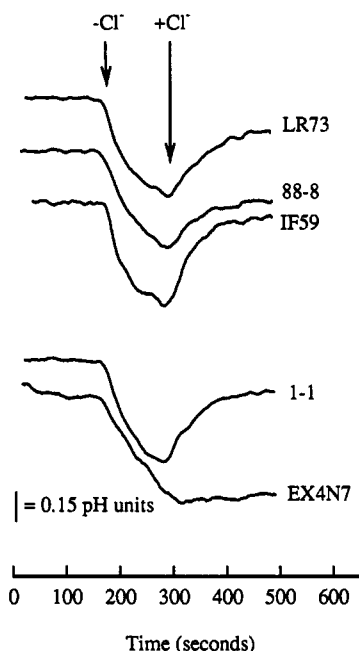


FIGURE 4: Cl^- substitution pH_i transients for the different cell lines performed in the absence of HCO_3^- . Each trace is the average of at least six individual experiments performed with six different cells from six different coverslips. Traces are unscaled, but are offset relative to each other for display purposes. Cells were loaded with BCECF as described in Materials and Methods and perfused at a constant rate (about 6 mL/min) with HBS (140 mM NaCl/5 mM KCl/2 mM CaCl_2 /1 mM MgCl_2 /10 mM glucose/10 mM HEPES, pH 7.30) in a specially constructed perfusion cell. Perfusate was changed from HBS with 150 mM Cl^- , pH 7.3, to HBS with 150 mM glutamate, pH 7.3, at the first arrow (very similar data are obtained by switching to gluconate, not shown) and then back to HBS with 150 mM Cl^- , pH 7.3, at the second arrow, 2 min after Cl^- removal. Recovery from acidosis still occurs if cells are exposed to Cl^- -free conditions for longer times, but we initially wished to keep this exposure as short as possible in order to treat the cells as gently as possible. Note the conspicuously slower recovery of the EX4N7 line from the mild acidosis induced by Cl^- removal, relative to the other cell lines.

In the absence of HCO_3^- , upon replacing extracellular Cl^- with equimolar glutamate (similar data are obtained using gluconate; not shown), LR73 cells are quickly acidified by about 0.3 units (cf. Figure 4 top trace, first arrow). This acidification begins to plateau in about 100 s and is reversed upon switching back to perfusate that contains $[\text{Cl}^-]$ (second arrow). A similar pattern is seen for both the 88-8 and IF5/9 cell lines (Figure 4, second and third traces from top). Although difficult to appreciate in this panel, the 1-1 and 88-8 cell lines have a slightly reduced efficiency of recovery from acidosis upon replacing Cl^- , relative to LR73, whereas the IF5/9 line recovers slightly faster. A more dramatic effect is seen for EX4N7, which takes much longer to plateau (not shown) and which recovers very slowly.

To better analyze the significance of these differences, similar Cl^- substitution experiments were performed in the presence of HCO_3^- (see Methods) to assess the relative importance of both HCO_3^- and Cl^- for pH_i homeostasis in these cells (Figure 5). As can be seen when comparing these traces, the MDR cell lines (EX4N7 and 1-1) exhibit behavior that is distinctly unlike that exhibited by the drug sensitive parental line LR73, or the cell lines produced by transfection with MDR mutants unable to confer an MDR phenotype (88-8 and IF5/9; compare bottom two traces to top three in Figure 5). Upon removal of Cl^- the acidification of the wild type mu MDR 1 transfectants is much more extensive, and recovery of pH_i upon readdition of Cl^- is altered. These

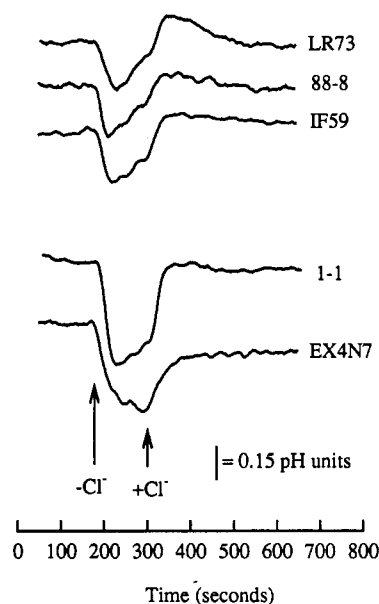


FIGURE 5: Cl^- substitution pH_i transients for the different cell lines performed in the presence of HCO_3^- . These experiments are essentially identical to those presented in Figure 4, except that the cells were perfused in HBSS (116 mM NaCl/5 mM KCl/10 mM glucose/24.2 mM NaHCO_3 /2 mM CaCl_2 /0.6 mM Na_2HPO_4 /1 mM MgCl_2 /0.5 mM KH_2PO_4) \pm Cl^- that was pre-equilibrated with 5% CO_2 (see Materials and Methods; note that $[\text{Cl}^-]_o$ in this case is 127 mM). Traces are unscaled, but offset relative to each other for display purposes. pH_o was verified for both buffers ($\pm \text{Cl}^-$) with a micro-electrode before use, and a fine jet of 5% CO_2 was directed over the surface of the perfusion chamber during the course of the experiments.

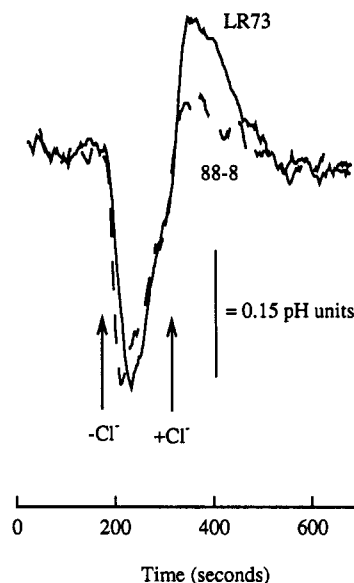


FIGURE 6: Expanded overlay of the LR73 (solid) and 88-8 (dashed) traces from Figure 5. Note that the traces are unscaled; however, since these cells have slightly different steady-state pH_i (Table 1), they are offset relative to each other. A LR73/IF59 overlay is similar (not shown), illustrating similar Cl^- and HCO_3^- pH_i homeostasis for these two cells (see Figure 5).

differences are better appreciated by examination of the expanded overlays presented in Figures 6–8. Note in particular the absence of any “overshoot” above initial steady-state pH_i during Cl^- -induced recovery for the MDR cells. Thus, we can immediately conclude that Cl^- - and HCO_3^- -dependent pH_i homeostasis is rather dramatically altered for the MDR cells.

To decipher the molecular basis of the differences between the traces in Figures 5–8, we followed several strategies

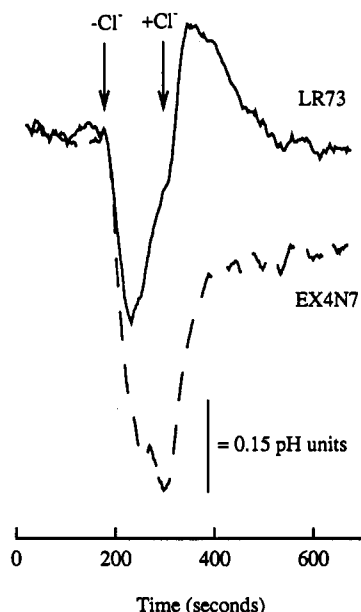


FIGURE 7: Expanded overlay of the LR73 (solid) and EX4N7 (dashed) traces from Figure 5.

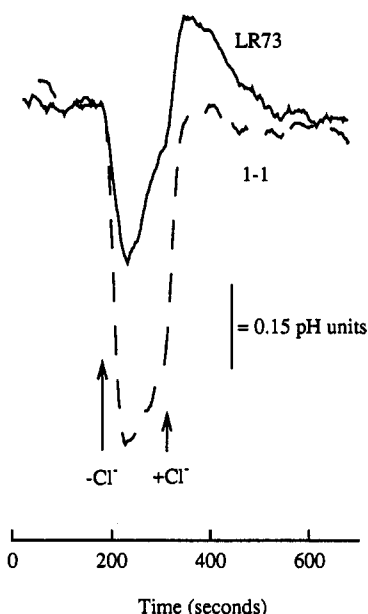


FIGURE 8: Expanded overlay of the LR73 (solid) and 1-1 (dashed) traces from Figure 5.

simultaneously. The first (see below) was a more detailed analysis of the ion dependencies of the components of the traces by performing similar experiments in the presence/absence of Na^+ to reveal $\text{Na}^+/\text{Cl}^-/\text{HCO}_3^-$ cotransport (Na^+/AE) and Na^+ -independent $\text{Cl}^-/\text{HCO}_3^-$ exchange (AE) processes [see Alpern and Chambers (1987) and Nord *et al.* (1988)], which likely add together to yield the observed complex behavior upon removing/replacing Cl^- in the presence of $-\text{HCO}_3^-$. The second (see below) was to analyze the effect of various inhibitors (e.g., stilbenes) in an attempt to selectively inhibit AE and Na^+/AE , respectively. The third was simply to subtract the traces. That is, we assume that the MDR cells have either lost or gained a Cl^- - and $-\text{HCO}_3^-$ dependent process that the parental cells do or do not have. Qualitatively, this process is revealed by subtraction of the traces. In Figure 9 (solid line), we present the result obtained upon subtracting the EX4N7 trace from the LR73 trace presented in Figures 5 and 7. The resultant LR73 minus EX4N7 difference trace

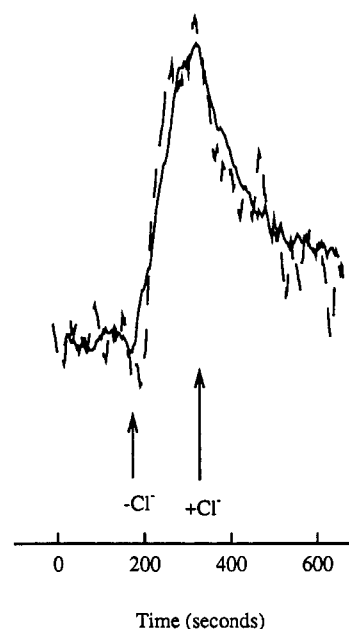


FIGURE 9: Comparison of the result produced by subtracting the EX4N7 trace from the LR73 trace presented in Figure 5 (solid line) to the result from a Cl^- substitution experiment performed for LR73 in the presence of $-\text{HCO}_3^-$ but the absence of Na^+ (dashed line; trace shown is representative of three experiments). In the Na^+ -free experiment, LR73 cells were initially perfused with normal HBSS. After 5-min equilibration, HBSS containing 141.4 mM Na^+ /5.5 mM K^+ was replaced with HBSS containing 146.9 mM K^+ /0 mM Na^+ . An instantaneous mild acidification (0.04 units) was observed, but pH_i was reasonably stable thereafter (a similar result is obtained upon replacing Na^+ with *N*-methyl-D-glucamine cation (not shown); a more detailed comparison of K^+ vs NMG^+ experiments will be published elsewhere). After 5-min equilibration, $\text{Cl}^-/\text{glutamate}$ exchange was performed, and 2 min later, Cl^- was replaced. Note the very similar rates of alkalization in the two traces, and the very similar rates of recovery. In other experiments involving longer incubation times in Cl^- -free buffer (not shown), the alkalization for LR73 cells in the absence of Na^+ is seen to completely plateau in about 3 min (the presented experiment involved 2-min exposure to Cl^- -free buffer in order to be consistent with the data presented in Figure 5). Note that the difference trace was scaled relative to the Na^+ -free LR73 trace (the difference trace was divided by about a factor of 1.5) to visually highlight the similarity in alkalization kinetics. Assuming similar buffering capacity for the two cells, and assuming that the Na^+ -free Cl^- substitution experiment reveals total AE activity for LR73 under these perturbations (which may be optimistic), we estimate that virtually all LR73 AE 2 activity is lost in EX4N7 (note that this is likely an oversimplification). More experiments are required to more precisely quantitate relative percent loss of AE 2 activity for the different MDR cell lines.

illustrates what is apparently lost from LR73 cells, with respect to Cl^- - and $-\text{HCO}_3^-$ -dependent pH_i homeostasis, upon transfection with wild type mu MDR 1. Importantly, selection was on G418 only for EX4N7. This was verified to lead to increased expression of mu MDR 1 mRNA and protein in the same cell cultures used for these experiments (not cells grown months apart that may have different characteristics, cf. Figure 2). Conspicuously and most interestingly, the difference trace (solid line) looks similar to what is expected in a Cl^- substitution experiment for a cell that harbors a $\text{Cl}^-/\text{HCO}_3^-$ exchanger (i.e., AE that is Na^+ -independent) but not a Na^+ -coupled AE [e.g., see Kopito *et al.* (1989) and Lee *et al.* (1991)]. That is, it appears as if the MDR cells have lost AE activity that normally exists in the LR73 parent (formally, they may have gained the thermodynamic converse, see Discussion). To verify this, and to examine whether the kinetics of the difference trace are consistent with AE that may occur in these cells under these conditions, we also present in Figure 9 (dashed

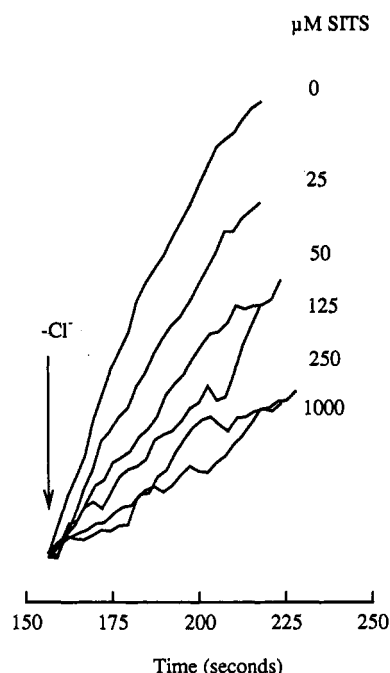


FIGURE 10: Alkalinization induced by Cl^- /glutamate exchange for LR73 cells perfused with Na^+ -free HBSS harboring various concentrations of SITS. Cells were perfused with HBSS/SITS for 3 min before Cl^- /glutamate exchange. Data from individual cells are smoothed as in Figure 3. IC_{50} for SITS calculated from these data is approximately $45 \mu\text{M}$, suggesting the presence of the AE 2 isoform (see also Figure 11).

line) the result of a Cl^- substitution experiment for LR73 cells performed in the presence of $-\text{HCO}_3^-$ but the absence of Na^+ [i.e., we reveal that component of the overall Cl^- substitution pH_i transient that is Na^+ -independent, but still Cl^- - and $-\text{HCO}_3^-$ -dependent; thus, we reveal AE; see, for example, Madhus and Olsnes (1987)]. Conspicuously, the difference between the EX4N7 and LR73 Cl^- substitution traces obtained in the presence of Na^+ looks similar to the Na^+ -independent AE trace for the LR73 cells (kinetically, they are very similar); that is, it appears as if the MDR cells have indeed lost Cl^- / $-\text{HCO}_3^-$ exchange ability.

To further show that the Na^+ -independent Cl^- substitution trace for LR73 cells illustrates AE activity, we performed Cl^- substitution experiments in the absence of Na^+ and the presence of various concentrations of SITS, a potent inhibitor of AE 1 that is somewhat less active against AE 2 [see Lee *et al.* (1991)]. As shown in Figure 10 we inhibit the AE activity of LR73 cells [calculated as the initial rate of alkalinization upon Cl^- removal, see Lee *et al.* (1991)] by about 50% at $50 \mu\text{M}$ SITS (apparent $\text{IC}_{50} = 45 \mu\text{M}$). This low sensitivity to stilbene is reminiscent of that seen previously for AE 2 in 293 cells transfected with murine AE 2 cDNA (Lee *et al.*, 1991). Thus, in the LR73 Na^+ -free experiment we are likely witnessing apparent AE 2 activity.

To further test this, and to examine whether the decrease in AE 2 activity for the MDR cells is due to altered expression of AE isoforms, as described previously (Roepe *et al.*, 1993) we performed quantitative northern blot analysis using isoform-specific AE probes. Parts A and B of Figure 11 present the results obtained upon probing purified mRNA from these cells with an AE 1 or an AE 2 cDNA fragment, respectively. Quantitation of the signals is accomplished by scanning the blot with a Betagen scanner and normalizing the AE signals to those for both β -actin and acidic ribophosphoprotein (rPO) mRNA, as described previously (Roepe *et al.*, 1993).

Remarkably, although by analysis of the Cl^- substitution traces a dramatic apparent decrease in AE 2 activity occurs in the EX4N7 and 1-1 MDR cells, relative expression of AE 1 and AE 2 mRNA is either constant or increased. Similar to previous data obtained with MDR myeloma cells (Roepe *et al.*, 1993), even though there is no expression of AE 1 in the parental cell line, we find a conspicuous band to which the AE 1 probe hybridizes in two of the MDR transfectants (1-1 and IF5/9; note that the AE 1 probe does not hybridize to AE 2 mRNA), suggesting that there is rather dramatic overexpression of a 3.5-kb AE 1 mRNA in the two drug-selected lines. Again similar to previous data (Roepe *et al.*, 1993) this 3.5-kb band is smaller than AE 1 transcripts isolated from other sources [see Lux *et al.* (1989) and Tanner *et al.* (1988)]; however, since the open reading frame of the AE 1 mRNA is only 2.8 kb, the size of this transcript is sufficient to encode the protein. Since antibodies specific to AE 2 or antibodies that are capable of distinguishing between AE 1 and AE 2 are unavailable, we are currently unable to distinguish between isoforms in immunoprecipitation experiments. Further examination of AE overexpression in these, and other, MDR cells will be published elsewhere. Note also the interesting appearance of a 4.4-kb AE 1 mRNA for EX4N7.

DISCUSSION

Previously (Roepe *et al.*, 1993), we suggested that Cl^- / $-\text{HCO}_3^-$ exchange was inhibited in a series of MDR myeloma cells, since Cl^- -dependent reacidification following an alkaline pH_i shock was impaired. In addition, decreased efficiency of reacidification appeared to be related to relative expression of MDR protein, which was also related to relative alkalinization of pH_i . In this previous work we were surprised to find increased AE 2 and AE 1 mRNA in some MDR cells; that is, the MDR cells, paradoxically, exhibited decreased apparent AE activity but increased AE mRNA. The data in this paper are analogous to this paradox; that is, although apparent AE 2 activity is decreased in MDR cells expressing functional MDR protein, apparent anion exchanger expression is either elevated or constant. Similarly, we find that expression of Na^+/H^+ exchanger in these cells is either constant or very mildly elevated [data not shown; see Roepe *et al.* (1993)]. Therefore, it is logical to conclude that MDR protein overexpression either directly or indirectly inhibits Na^+ -independent anion exchange (AE) in these cells. Inhibition of AE (which is net acidifying) might help to explain why pH_i is elevated in many MDR cells. Although more exotic models can be envisioned, one tantalizing possibility is that the anion conductance mediated by MDR protein (Valverde *et al.*, 1992; Gill *et al.*, 1992; Altenberg *et al.*, 1994) is, in some fashion, responsible for this perturbation.

Thus, this led us to examine Cl^- - and $-\text{HCO}_3^-$ -dependent pH_i homeostasis in these transfected LR73 cells by the more rigorous method of single-cell photometry. Since some members of this series were created without selection on chemotherapeutic drug, an additional level of complexity was eliminated, and we could in addition compare and contrast the data to similar data obtained with cell lines harboring mutant MDR proteins. These new data may be summarized as follows:

1. MDR cells created by transfecting CHO fibroblasts with wild type mu MDR 1 cDNA exhibit pH_i 0.13–0.34 units higher than the parental line, whereas a cell line expressing similar amounts of mutant MDR protein that is unable to confer the MDR phenotype, as well as a revertant wild type transfectant, exhibit pH_i similar to the parent's. EX4N7 was

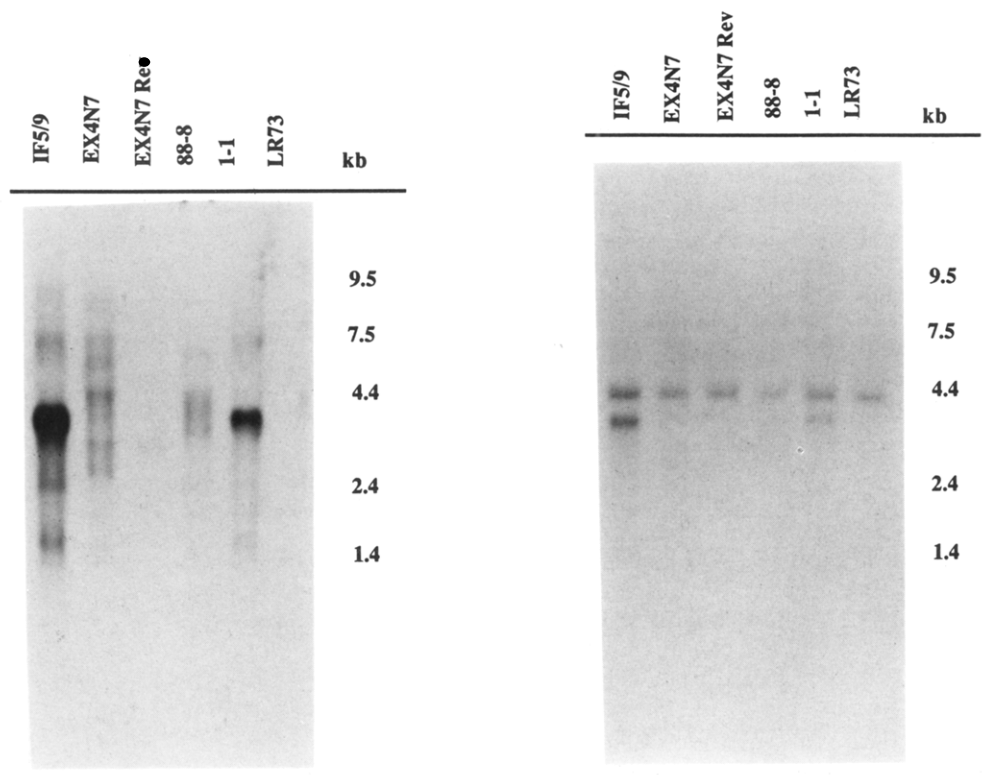


FIGURE 11: Northern blot analysis of AE 1 (A, left) and AE 2 (B, right) expression in the series of cell lines performed as described previously (Roepe *et al.*, 1993). Each lane harbors 5 μ g of purified mRNA. Note that repeated stripping of the blot presented in panel A was unable to completely remove the strong AE 1 signal, which is still partially apparent in B (the smaller band at about 3.5 kb); nonetheless, the AE 2 probe is specific for AE 2 [see Roepe *et al.* (1993)]. In any case, note the much stronger signal obtained with the AE 1 probe (which harbored similar cpm/ng cDNA; similar amounts of probe were used in both blots, and both blots were exposed for 14 h) indicating significant overexpression of 3.5-kb AE 1 mRNA, that apparently only occurs upon selection in chemotherapeutic drug. Note that the other faint bands in this blot likely reveal other transcripts that are frequently seen for AE expressing cells (Alper *et al.*, 1988; Kudrycki *et al.*, 1990). Quantitation of the AE 2 signals in B allows us to estimate the AE 2 is mildly overexpressed for the IF5/9 cell line (2–2.5-fold), relative to LR73, but expressed to very similar levels in LR73, 1-1, and EX4N7. Essentially identical data were obtained with a second blot using different mRNA preparations (not shown).

not found to overexpress Na⁺/H⁺ exchanger (NHE, data not shown), although the 1-1 line may overexpress NHE very slightly as found previously for other MDR cells (Roepe *et al.*, 1993). EX4N7 also harbors 3–4-fold more p-GP 1 mRNA relative to the other cells (data not shown); thus rigorously we cannot exclude the possibility that a small amount of hamster MDR 1 protein contributes to the EX4N7 phenotype.

2. EX4N7 and 1-1 MDR cells also exhibit decreased $\Delta\Psi$, similar to previously examined MDR myeloma cells (Roepe *et al.*, 1993). Cells harboring a crippled MDR mutant (IF5/9) curiously exhibit slightly elevated pH_i and $\Delta\Psi$. Whether these alterations, or others caused by vinblastine selection, lead to the exhibited vinblastine resistance remains to be determined.

3. Elevated pH_i is due at least in part to altered Cl⁻ and HCO₃⁻-dependent pH_i homeostasis, as concluded previously for MDR myeloma cells (Roepe *et al.*, 1993). Specifically, it appears that AE 2 mediated Cl⁻/HCO₃⁻ exchange is reduced in the cells expressing functional mu MDR 1 protein but not mutant MDR protein. Decreased AE activity is not due to decreased AE expression; thus, an attractive possibility is that it is caused by MDR protein. Increased AE 1 expression may be a frequent event in MDR cells [see also Roepe *et al.* (1993)].

It is unlikely that a mutated and/or overexpressed Na⁺/Cl⁻/HCO₃⁻ cotransporter causes pH_i changes in these MDR cells. Although the cotransporter is net alkalizing, selection on G418 (see data for EX4N7) would have to cause the mutation and/or overexpression, which seems unlikely. Also, differences in Cl⁻ and HCO₃⁻-dependent pH_i homeostasis between these cells are largely Na⁺ independent (P. D. Roepe,

J. Weisburg, J. G. Luz, M. Hoffman, and L.-Y. Wei, unpublished).

These data are consistent with an evolving model for MDR protein function wherein the perhaps incompletely defined ion-translocating ability of the protein alters pH_i and $\Delta\Psi$, which then leads indirectly to altered sequestration and intracellular partitioning of chemotherapeutics.² Whether or not the model is correct, the logic behind it is also important with respect to other models (Gill *et al.*, 1992) that envision the protein to function as *both* an ion and drug transporter. The model predicts complex and heterogeneous behavior for different cell types with regard to drug resistance, since different MDR cells express different levels and isoforms of NHE and AE [see also Roepe *et al.* (1993)] and have different resting $\Delta\Psi$ and pH_i. Thus, the IF5/9 cell line, which overexpresses AE 1 along with crippled MDR 1 and which has mildly elevated pH_i and $\Delta\Psi$, is mildly resistant to vinblastine but not doxorubicin or colchicine. It should prove interesting to separate the contributions $\Delta\Psi$ and pH_i make

² Although many reports have associated elevated pH_i with MDR, one recent report has measured lowered pH_i for a doxorubicin-selected cell line (Altenberg *et al.*, 1993). Also in this work a MDR transfectant that was subsequently selected on doxorubicin was found to exhibit a pH_i similar to that of the parent. Although we have no simple explanation for this one apparent discrepancy, as shown in this work (cf. Figure 2) transfectants can easily revert. Resistance to one or more drugs is no guarantee of p-GP mediated MDR [see Cole *et al.* (1992)]; thus we feel that a detailed examination of MDR protein expression in cells used to measure pH_i is warranted (even for transfectants, see Figure 2). It should also prove interesting to measure $\Delta\Psi$ for other MDR cells, as well as relative expression of AE isoforms.

individually to drug resistance from others promoted by selection on chemotherapeutic. It will also be advantageous to more completely understand the effects $\Delta\Psi$ have on partitioning of these compounds, including detailed analysis of rates of passive diffusion of the neutral and charged forms.

The molecular level details explaining how overexpression of MDR protein lowers $\Delta\Psi$ (presumably by increasing Cl^- permeability) and raises pH_i (presumably by inhibiting AE) in at least two different cell types [i.e., myeloma cells (Roepe *et al.*, 1993) and these fibroblasts] are yet to be completely worked out; however, these new data, along with other recent work (Cordon-Cardo *et al.*, 1990; Valverde *et al.*, 1992; Stutts *et al.*, 1993) suggest some interesting possibilities:

1. MDR protein is a Cl^- channel (as originally proposed by Higgins, Sepúlveda, and colleagues) that directly lowers $\Delta\Psi$ and then indirectly alters pH_i . The indirect effect on pH_i could be due to several different mechanisms, one perhaps being that decreased $\Delta\Psi$ alters the efficiency of normal AE 2 mediated anion exchange for some cells. Although net exchange by an electroneutral exchanger is presumably unaffected by $\Delta\Psi$, individual steps of the catalytic cycle can be affected (Jennings *et al.*, 1990); in particular, in the presence of divalent anions, lower $\Delta\Psi$ can decrease association of Cl^- to the external AE 1 binding site.

2. MDR protein is an electrogenic anion exchanger or cotransporter that directly affects both $\Delta\Psi$ and pH_i in the observed fashion. This is formally possible, since previously published Cl^- conductance measurements are actually anion conductance measurements performed in the absence of $^-\text{HCO}_3$. Recall also that, at least in the case of AE 1, anion exchangers are capable of Cl^- conductance (10^5 ions/s) that approaches that exhibited by channels.

Although it is unusual, we suggest model 2 because of the known tissue distribution of MDR protein and the known physiology of those tissues (Cordon-Cardo *et al.*, 1990). One conspicuous site of endogenous MDR 1 expression is the luminal face of the kidney proximal tubule. Various mathematical models have been used to better understand trans-cellular flow of Cl^- and $^-\text{HCO}_3$ as well as volume and pH_i regulation in these cells [see Weinstein (1986, 1992) and Preisig and Alpern (1989)]. One model (Weinstein, 1992) uses a recently postulated $\text{Cl}^-/\text{H}_2\text{CO}_2$ exchange process (Karniski & Aronson, 1987) to explain some features of pH_i regulation and observed Cl^- flux that are difficult to model otherwise. An electrogenic exchanger in the luminal membrane is also energetically consistent with Cl^- transport in proximal tubule (Alan Weinstein, personal communication), whereas although a Cl^- channel could function as a volume "safety valve" for these cells, its presence on the luminal face is less consistent with observed Cl^- flux.

By demonstrating that MDR protein may inhibit AE, we are better able to explain elevated pH_i for many (if not most) MDR cells. However, it is not immediately apparent to us how any simple ion-transport process (channel, exchanger, or cotransporter) would directly lead to the decrease in apparent AE activity observed in these LR73 cells. Thus, further studies that investigate the effects of $\Delta\Psi$ on AE 2 function and the consequences of altered $[\text{Cl}^-]_i$ and Cl^- permeability in different eukaryotic cell types, as well as the role MDR protein ATPase activity plays in ion transport, will be valuable with respect to refining models.

Aside from providing mechanistic clues, these data also highlight the potential complexities of the basic MDR phenotype. Namely, the altered expression of known anion exchangers in these and other MDR cells (Roepe *et al.*, 1993)

suggests that some MDR cells may attempt to compensate for the unusual Cl^- (and perhaps $^-\text{HCO}_3$) transport instigated by the overexpression of MDR protein by significantly altering their expression of other anion transporters as well. This makes continued analysis of the differences in Cl^- - and $^-\text{HCO}_3$ -dependent pH_i homeostasis for MDR cells a more detailed, yet perhaps more fruitful endeavor.

ACKNOWLEDGMENT

The authors thank Dr. Phillippe Gros, McGill University, for generously providing the cell lines used in this work and for advice and encouragement. They also thank Shailesh Parmar for help with tissue culture and Drs. Randi Silver, Olaf Andersen, Alan Weinstein, and Larry Palmer (Cornell University Medical College) and Dr. James O'Brien (Sloan-Kettering Institute) for helpful discussion. They also thank Dr. Joseph Bertino, Sloan-Kettering Institute, for allowing them to modify his laboratory's P.T.I. alphascan for these experiments, Carl Pfaff of the Sloan-Kettering Medical Physics laboratory for advice in constructing the S.C.P. perfusion chamber, and Dr. Ron Kopito (Stanford University) for providing AE 1 and AE 2 cDNAs. This research was performed in the Sackler Laboratory of Membrane Biophysics at the Sloan-Kettering Institute. P.D.R. is a Sackler Scholar at MSKCC.

REFERENCES

- Alper, S., Kopito, R. R., Libresco, S. M., & Lodish, H. F. (1988) *J. Biol. Chem.* 263, 17092–17099.
- Alpern, R. J., & Chambers, M. (1987) *J. Gen. Physiol.* 89, 581–598.
- Altenberg, G. A., Young, G., Horton, J. K., Glass, D., Belli, J. A., & Reuss, L. (1993) *Proc. Natl. Acad. Sci. U.S.A.* 90, 9735–9738.
- Altenberg, G. A., Deitmer, J., Glass, D. C., & Reuss, L. (1994) *Cancer Res.* 54, 618–622.
- Ames, G. F.-L. (1986) *Annu. Rev. Biochem.* 55, 397–425.
- Azzaria, M., Schurr, E., & Gros, P. (1989) *Mol. Cell. Biol.* 9, 5289–5297.
- Beck, W. T. (1987) *Biochem. Pharmacol.* 36, 2879–2887.
- Biedler, J. L., & Rheim, H. (1970) *Cancer Res.* 30, 1174–1184.
- Boscoboinik, D., Gupta, R. S., & Epand, R. M. (1990) *Br. J. Cancer* 61, 568–572.
- Chomczynski, P., & Sacchi, N. (1987) *Anal. Biochem.* 162, 156–159.
- Cole, S. P. C., Bhardwaj, G., Gerlach, J. H., Mackie, J. E., Grant, C. E., Almquist, K. C., Stewart, A. J., Kurz, E. U., Duncan, A. M. V., & Deeley, R. G. (1992) *Science* 258, 1650–1654.
- Cordon-Cardo, C., O'Brien, J. P., Boccia, J., Casals, D., Bertino, J. R., & Melamed, M. R. (1990) *J. Histochem. Cytochem.* 38, 1277–1287.
- Dalton, W. S., Grogan, T. M., Rybski, J. A., Scheper, R. J., Richter, L., Kailey, J., Broxterman, H. J., Pinedo, H. M., & Salmon, S. E. (1989) *Blood* 73, 747–752.
- Devault, A., & Gros, P. (1990) *Mol. Cell. Biol.* 10, 1652–1663.
- Devine, S. E., Hussain, A., Davide, J. P., & Melera, P. W. (1991) *J. Biol. Chem.* 266, 4545–4555.
- Endicott, J. A., & Ling, V. (1989) *Annu. Rev. Biochem.* 58, 137–171.
- Gill, D. R., Hyde, S., Higgins, C. F., Valverde, M. A., Mintenig, G. M., & Sepúlveda, F. V. (1992) *Cell* 71, 23–32.
- Gottesman, M. M., & Pastan, I. (1988) *J. Biol. Chem.* 263, 12163–12166.
- Gros, P., Dhir, R., Croop, J., & Talbot, F. (1991) *Proc. Natl. Acad. Sci. U.S.A.* 88, 7289–7293.
- Hammond, J. R., Johnstone, R. M., & Gros, P. (1989) *Cancer Res.* 49, 3867–3871.

- Higgins, C. F., Hyde, S. C., Mimmack, M. M., Gileadi, U., & Gill, D. R. (1990) *J. Bioenerg. Biomembr.* 22, 571–592.
- Homolya, L., Holló, Z., Germann, U. A., Pastan, I., Gottesman, M. M., & Sarkadi, B. (1993) *J. Biol. Chem.* 268, 21493–21496.
- Iversen, J. G. (1976) *J. Cell Physiol.* 89, 267–276.
- Jennings, M. L., Allen, M., & Schult, R. K. (1990) *J. Gen. Physiol.* 96, 991–1012.
- Kachel, V. (1990) in *Flow Cytometry and Sorting*, 2nd ed., pp 45–80, Wiley-Liss Inc., New York.
- Karniski, L. P., & Aronson, P. S. (1987) *Am. J. Physiol.* 253, F513–F521.
- Keizer, H. G., & Joenje, H. (1989) *J. Natl. Cancer Inst.* 81, 706–709.
- Kopito, R. R., Lee, B. S., Simmons, D. M., Lindsey, A. E., Morgans, C. W., & Schneider, K. (1989) *Cell* 59, 927–937.
- Kudrycki, K. E., Newman, P. R., & Schull, G. E. (1990) *J. Biol. Chem.* 265, 462–471.
- Laris, P. C., & Hoffman, J. F. (1986) in *Optical Methods in Cell Physiology* (DeWeer, P., & Salzberg, B. M., Eds.) pp 199–210, Wiley-Interscience Inc., New York.
- Lee, B. S., Gunn, R., & Kopito, R. R. (1991) *J. Biol. Chem.* 266, 11488–11494.
- Loew, L., Cohen, L. B., Dix, J., Fluhler, E. N., Montana, V., Salama, G., & Wu, J.-y. (1993) *J. Membr. Biol.* (in press).
- Lux, S. E., John, K. M., Kopito, R. R., & Lodish, H. F. (1989) *Proc. Natl. Acad. Sci. U.S.A.* 86, 9089–9093.
- Madhus, I. H., & Olsnes, S. (1987) *J. Biol. Chem.* 262, 7486–7491.
- Montana, V., Farkas, D. L., & Loew, L. M. (1989) *Biochemistry* 28, 4536–4539.
- Nord, E. P., Brown, S. E. S., & Crandall, E. D. (1988) *J. Biol. Chem.* 263, 5599–5606.
- Preisig, P. A., & Alpern, R. J. (1989) *J. Clin. Invest.* 83, 1859–1867.
- Prochaska, H., & Santamaria, A. B. (1988) *Anal. Biochem.* 169, 328–336.
- Roepe, P. D. (1992) *Biochemistry* 31, 12555–12564.
- Roepe, P. D., Carlson, D., Scott, H., & Wei, L.-Y. (1992) *J. Gen. Physiol.* 100, 52a.
- Roepe, P. D., Wei, L.-Y., Cruz, J., & Carlson, D. (1993) *Biochemistry* 32, 11042–11056.
- Roos, A., & Boron, W. F. (1981) *Physiol. Rev.* 61, 296–434.
- Rottenberg, H. (1979) *Methods Enzymol.* 55, 547–569.
- Sambrook, J., Fritsch, E. F., & Maniatis, T. (1989) *Molecular Cloning: A Laboratory Manual*. Cold Spring Harbor Laboratory Press, Cold Spring Harbor.
- Savitzky, S., & Golay, G. (1964) *Anal. Chem.* 36, 1627–1639.
- Stutts, M. J., Gabriel, S. E., Olsen, J. C., Gatzky, J. T., O'Connell, T. L., Price, E. M., & Boucher, R. C. (1993) *J. Biol. Chem.* 268, 20653–20658.
- Tanner, M. J. A., Martin, P. G., & High, S. (1988) *Biochem. J.* 256, 703–712.
- Thiebaut, F., Currier, S. J., Whitaker, J., Haugland, R. P., Gottesman, M. M., Pastan, I., Willingham, M. C. (1990) *J. Histochem. Cytochem.* 38, 685–690.
- Thomas, J. A., Buchsbaum, R. N., Fimniak, A., & Racker, S. (1979) *Biochem. J.* 18, 2210–2218.
- Tonnessen, T. I., Sandvig, K., & Olsnes, S. (1990) *J. Gen. Physiol.* C1117–C1126.
- Valverde, M., Diaz, M., Sepúlveda, F. V., Gill, D. R., Hyde, S. C., & Higgins, C. F. (1992) *Nature* 355, 830–833.
- Wei, L.-Y., & Roepe, P. D. (1994) *Biochemistry* (preceding paper in this issue).
- Weiner, I. D., & Hamm, L. L. (1990) *J. Clin. Invest.* 85, 274–281.
- Weinstein, A. M. (1986) *Am. J. Physiol.* 250, F860–F873.
- Weinstein, A. M. (1992) *Am. J. Physiol.* 263, F784–F798.